

Valence band modification of Cr₂O₃ by Ni-doping: Creating a high figure of merit p-type TCO

Elisabetta Arca,^{1, a)} Aoife B. Kehoe,² Tim D. Veal,³ Aleksey Shmeliov,² David O. Scanlon,^{4, 5} Clive Downing,² Dermot Daly,² Daragh Mullarkey,¹ Igor Shvets,¹ Valeria Nicolosi,² and Graeme W. Watson²

¹⁾ *School of Physics and CRANN, Trinity College Dublin, Dublin, Ireland*

²⁾ *School of Chemistry and CRANN, Trinity College Dublin, Dublin, Ireland*

³⁾ *Stephenson Institute for Renewable Energy and Department of Physics, School of Physical Sciences, University of Liverpool, L69 7ZF, UK*

⁴⁾ *University College London, Kathleen Lonsdale Materials Chemistry, Department of Chemistry, 20 Gordon Street, London WC1H 0AJ, UK*

⁵⁾ *Diamond Light Source Ltd., Diamond House, Harwell Science and Innovation Campus, Didcot, Oxfordshire OX11 0DE, UK*

^{a)} Electronic mail: earca@tcd.ie; Present address: National Renewable Energy Laboratory, 15013 Denver West Parkway, Golden, Colorado 80401, United States

I. SUPPORTING INFORMATION

A. TEM

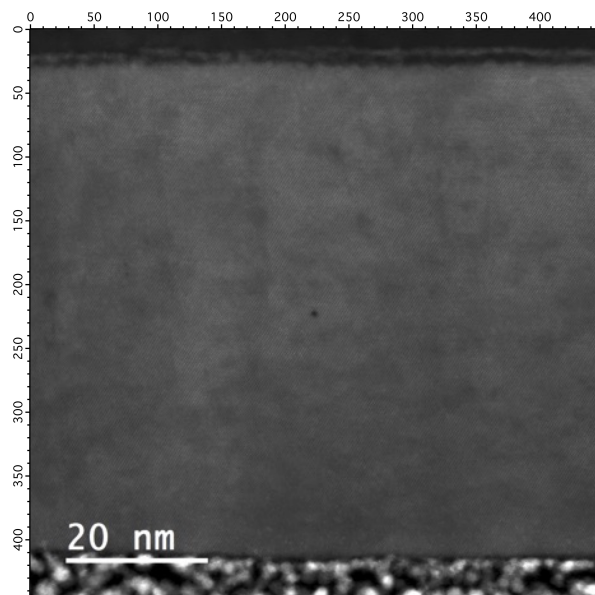


FIG. 1. ADF STEM image of Ni doped Cr₂O₃ lamella along [100] direction. Pt deposited on the surface of Cr₂O₃ during lamellae preparation can be seen at the bottom of the image.

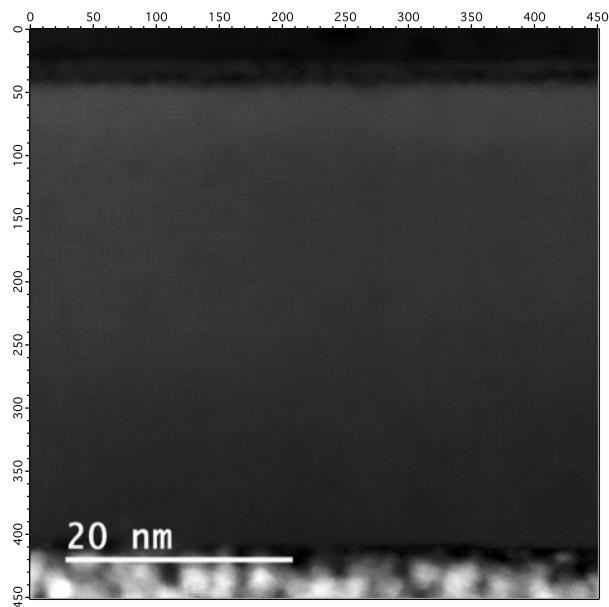


FIG. 2. ADF STEM image of Mg doped Cr₂O₃ lamella along [210] direction. Pt deposited on the surface of Cr₂O₃ during lamellae preparation can be seen at the bottom of the image.

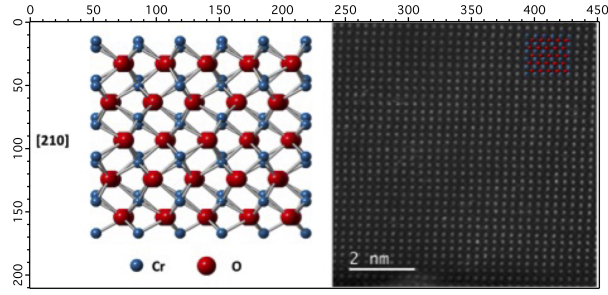


FIG. 3. (a) Structure of Cr_2O_3 along $[210]$ direction. (b) ADF STEM images of Mg doped Cr_2O_3 lamella.

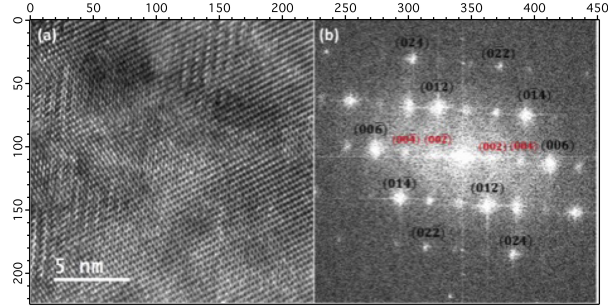


FIG. 4. (a) HRTEM image of Ni doped Cr_2O_3 lamella along $[100]$ direction with corresponding (b) its Fast Fourier Transform. The spots marked red are forbidden reflections.

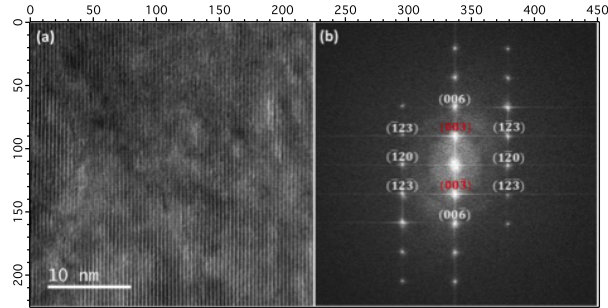


FIG. 5. (a) HRTEM image of Mg doped Cr_2O_3 lamella along $[210]$ direction with corresponding (b) FFT. The spots marked red are forbidden reflections.

B. XPS

The Ni 3p and Cr 3s region was peak fitted with the peak positions determined as indicated in Table I

The Ni content was determined using XPS according to:

$$\text{Ni content} = \text{Effective Ni 3p peak area} / (\text{Effective Ni 3p peak area} + \text{Effective Cr 3s peak area})$$

where the effective Cr 3s and Ni 3p peak areas are those which include the satellite features and are divided by the relative sensitivity factor (RSF) for the particular orbital (0.596 for Cr 3s and 2.22 for Ni 3p). The Cr 3s and Ni 3p peaks were chosen as they have very similar binding energies and so very similar kinetic energies and inelastic mean free paths. As a result, they both correspond to the same effective probing depth. The inelastic mean free paths were estimated to be 3 nm using the Tanuma, Powell and Penn TPP-2M formula [1] as implemented in the NIST software [2,3]

TABLE I. The XPS peak positions determined by curve fitting.

XPS line	Binding Energy (eV)
Ni 3p _{3/2}	66.7
Ni 3p _{3/2}	68.4
Ni 3p sat	70.7
Cr 3s	74.3
Cr 3s sat	78.4

- 1, S. Tanuma, C. J. Powell, and D. R. Penn, Surf. Interface Anal. **21**, 165 (1994)
- 2, C. J. Powell and A. Jablonski, NIST Electron Inelastic-Mean-Free-Path Database - Version 1.2, National Institute of Standards and Technology, Gaithersburg, MD (2010).
- 3, <https://www.nist.gov/srd/nist-standard-reference-database-71>

TABLE II. The analysis of the peak areas to determine the Ni content in the films.

Sample nominal Ni content	total Cr 3s area	Cr 3s area /RSF	total Ni 3p area	Ni 3p area /RSF	XPS Ni content
12%	1520	2550	742	334	11.6%
10%	478	802	190	86	9.7%

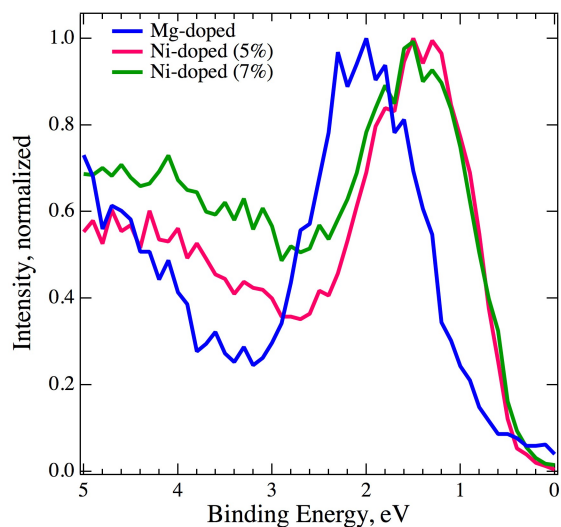


FIG. 6. Valence band maximum of one film doped with Mg (6%) and two doped with respectively 5% and 7% Ni. The binding energy scales were all referenced by aligning the signal from the aliphatic carbon 1s peak to 285 eV